UDC 612.8
DOI: 10.15587/2519-4798.2023.275390

SONOELASTOGRAPHIC EVALUATION OF SALIVARY GLAND LESIONS WITH CLINICOPATHOLOGICAL ASSOCIATION

Arpit Deriya, Deepti Arora, Ankur Malhotra, Shruti Chandak, Vaibhav Goyal, Paurush Jain

Sonoelastography is a comparatively new and developing technology in the field of salivary gland imaging. Nevertheless, it has the potential to distinguish between various types of lesions by calculating the degree of strain-related deformation under the externally applied force. With this background, the present study was undertaken to evaluate the role of sonoelastography in characterising salivary gland lesions as benign or malignant.

The aim: *To evaluate and characterize salivary Gland lesions on the Gray scale and Colour doppler ultrasonography and sonoelastography and to correlate these findings with the clinico-pathological diagnosis.*

Methodology: *This prospective cross-sectional study was conducted in the Department of Radiodiagnosis, Teerthanker Mahaveer Medical College & Research Centre, Moradabad (U.P.), from Aug 2021 to Nov 2022. All patients referred to the radiology department for imaging with clinical suspicion of having salivary gland lesions were enrolled in the study and evaluated on the SIEMENS ACUSON S3000 machine. Gray scale USG was done first to assess various morphological features of lesions, and then a Doppler assessment was done to determine vascularity within the lesion. Subsequently, real-time strain elastography (eSie touch) was performed to assess the tissue stiffness. The elastogram image of the detected lesions was evaluated using colour coding ranging from blue (soft) through green (intermediate/average hardness) and red (hard). After strain elastography, shear wave elastography of the lesion was also performed using Virtual Touch Quantification (VTQ) and Virtual Touch Imaging Quantification (VTIQ) software. The sonographic findings were correlated with histopathological diagnosis. The acquired data were subjected to statistical analysis using the software SPSS version 20. Sensitivity, specificity, PPV and NPV were calculated for conventional ultrasound techniques alone & in combination with elastography.*

Results: *Out of the 50 salivary gland lesions included in the study, 44 (88 %) were benign, whereas 6 (12 %) were malignant on cytology. The age of the study population ranged from 16 to 75 years, with a mean age of 38.82 years. Pleomorphic adenoma (60 %) was the most frequent lesion, followed by Warthin's tumour (28 %). The Conventional USG showed 66.67 %, sensitivity, 52.27 %, specificity, 16.00 %, PPV, 92.00 % NPV and 54.00 % accuracy in differentiating benign from malignant lesions while USG- Elastography combined showed higher diagnostic performance with 83.33 %, sensitivity, 79.55 %, specificity, 35.71 % PPV, 97.22 % NPV and 80.00 %, accuracy. The specific cut-off scores for the sonoelastography score, eSie touch, VTQ, and VTIQ were also determined to diagnose a lesion as malignant or benign, and the difference was found to be statistically significant.*

Conclusions: *Sonoelastography alone cannot be solely relied upon to distinguish between malignant & benign salivary gland abnormalities. However, it can be combined with conventional USG for better differentiation and characterization of these lesions*

Keywords: *salivary gland, ultrasonography, sonoelastography, strain elastography, shear elastography*

How to cite:
Deriya, A., Arora, D., Malhotra, A., Chandak, S., Goyal, V., Jain, P. (2023). Sonoelastographic evaluation of salivary gland lesions with clinicopathological association. ScienceRise: Medical Science, 1 (52), 10–20. doi: http://doi.org/10.15587/2519-4798.2023.275390

1. Introduction

Salivary gland tumours account for a significant proportion of oral and maxillofacial pathologic abnormalities [1]. Salivary gland diseases range in severity from mild inflammatory illnesses to a variety of benign-&-malignant neoplasms. Most salivary gland illnesses manifest as gland enlargement, and the preponderance of neoplasms originate in the parotid gland, with the remainder (10–15 %) occurring in the submandibular gland. It has been estimated that the annual incidence of salivary gland neoplasms is around 2.5–3 cases per 100,000 people [2, 3].

The management of a salivary gland lesion is primarily decided by whether the lesion is benign or malignant (type of histology of the lesion). Therefore, it is crucial to distinguish between benign-&-malignant salivary gland lesions before surgery since the latter may require more complex surgery [4, 5].

Although FNAC is the ideal preoperative diagnostic tool for salivary gland lesions, it is an invasive proce-

dure; hence non-invasive techniques are often used [6]. The radiological methods employed for imaging salivary gland lesions include ultrasound, computed tomography, and magnetic resonance imaging (MRI) [7].

B mode ultrasound is a sensitive and presently recommended first-line imaging tool for patients with salivary gland enlargement because it is non-invasive, radiation-free, simple to use, time and cost-effective, and provides good resolution for superficial tissues. The majority of the time, it is possible to display the lesion's precise position, size, shape, consistency, and margins. Additionally, ultrasound can properly determine if a lesion is intraglandular or extraglandular. However, because the morphological characteristics of benign-&-malignant-lesions frequently overlap, sometimes neither greyscale nor colour doppler ultrasonography can distinguish the nature of a tumour [8, 9].

More details regarding the mass and the structures around it (such as the mandible or temporal bone) can be obtained using CT and MRI. However, these procedures are time-consuming, costly, and not always accessible. Additionally, CT comes with an associated danger of radiation exposure [10]. Further, due to the substantial overlap in the imaging characteristics of benign-&-malignant salivary gland lesions, despite their great sensitivity, they cannot distinguish between benign-&-malignant-lesions [11].

Sonoelastography is a relatively modern technology that provides qualitative, quantitative, and semi-quantitative characteristics to quantify the elasticity of the tissue. The cornerstone behind this modality is the repetitive application of pressures to the tissue with an ultrasonic probe. Shear Wave Elasticity Imaging (SWEI) was first conceptually characterized by Sarvazyan et al. in 1998 [12] and realistically explored by Nightingale and Trahey in the period of 1995–2003 [13]. The physician's fingers on the surface of the body or organ are replaced by the radiation force, which functions as a "virtual finger" that can be employed to palpate the organ from within the organ [14].

Elastograms, also known as colour maps, quantify and illustrate changes in tissue displacement [14–16]. A cutting-edge method enables overlaying that colour scale with an elasticity score over the typical ultrasound image in greyscale. A separate colour is used to indicate each elasticity score [15, 17]. Soft tissue is represented by red, medium-stiff tissue by green, and "hard" tissue by blue. Grayscale sonograms are overlaid with colour-scaled elastograms to enable an examination of the elasticity of any visible lesions [16].

There is a paucity of sonoelastography research on the salivary gland in the Indian population, despite the fact that this approach has been proven effective in distinguishing benign from malignant lesions in breast, thyroid, and prostate cancer [18]. Due to the concomitant desmoplastic response, most malignant lesions are harder than benign lesions. Elastography, primarily based on this concept, distinguishes between various types of lesions by measuring the degree of strain-related deformation under the externally applied force [19].

Sonoelastography is a comparatively new and evolving technology in the field of salivary gland imaging [20]. To confirm and demonstrate its efficacy in salivary gland imaging, more research is still needed. With this background, the present study was undertaken to evaluate the diagnostic accuracy of sonoelastography in characterizing salivary gland lesions and to prospectively correlate it with conventional ultrasonography and clinicopathological diagnosis. Additionally, we believe that the inclusion of elastographic data to pre-existing Grayscale and Color doppler USG may improve the assessment of salivary gland lesions, thereby eliminating the need for additional MRI/CT scanning.

2. Materials and methods

This prospective cross-sectional study was conducted in the Department of Radiodiagnosis, Teerthanker Mahaveer Medical College & Research Centre, Moradabad (U.P.), from Aug 2021 to Nov 2022. This study was performed following ethical principles and standards for conducting medical research in India and was started after taking due approval from the ethical committee of TMU University (TMU/IEC/20-21/083 dated 28/07/2021) and written informed consent from patients.

All the patients who were referred to the radiology department for imaging with clinical suspicion of having salivary gland lesions and were incidentally found to be having salivary gland lesions on imaging were enrolled in the study. The lesions clearly outside the confines of the salivary gland on ultrasound were excluded from the study. Also, patients with a previous history of salivary gland surgery/malignancy/radiation therapy and patients who refused to give prior written consent/ Uncooperative patients were also excluded from the research.

Ultrasound was performed while a patient was lying in a supine position with the neck turned to the opposite side during the examination of the parotid gland, whereas imaging of the submandibular gland was performed in a hyperextended neck position. Gray Scale Ultrasound, Color Doppler and ultrasound elastography of the Salivary Gland Lesions were performed on SIEMENS ACUSON S3000 (Germany) machine using Siemens 9L4 linear-array probe (4-9MHz), and the findings were correlated with the clinical-pathological diagnosis.

The salivary gland lesions were carefully analyzed, and various sonomorphological features were recorded as follows [21–23] – Gland involved (Parotid/Submandibular/Both), Laterality (Unilateral/Bilateral), Focal/Diffuse Involvement, Size of the lesion (in the perpendicular plane in mm), the shape of the lesion (round/oval/lobulated/irregular), Margin of the lesion (Well demarcated/Poorly demarcated), consistency of lesion (Solid/Cystic/Mixed), Echo-pattern of the lesion (Anechoic/Hypoechoic/Isoechoic/Hyperechoic/Mixed) and Echo-texture of the lesion (Homogeneous/Heterogeneous). Doppler assessment was also done to evaluate the presence and pattern of vascularity within the lesion.

Subsequently, Sonoelastography was performed using a 9L4 linear array transducer of frequency 4–9 MHz with the same depth focus and gained settings as grayscale imaging. The scanner was switched to Elastographic mode (eSie touch), and real-time strain elastography was performed to assess the tissue stiffness. The Grayscale and sonoelastography images were pre-

sented side by side on a dual screen. Wherever possible, the elastographic window or box was positioned to encompass the whole tumour region, including some of the healthy surrounding tissue, and the box size was modified accordingly. Patients were instructed to hold their breath while recording measurements. The quality of the elastography was indicated by the quality factor, which was kept at 65 [24].

The elastogram image of the detected lesions was evaluated using colour coding ranging from blue (soft) through green (intermediate/average hardness) and red (hard). In addition, all lesions were scored on elastogram in terms of their stiffness and compared to normal parenchyma using a 4-grade system as follows [10].

Score 1 – The lesion has elasticity similar to the surrounding glandular parenchyma (soft).

Score 2 – The lesion is predominantly soft compared to the adjacent parenchyma, with some areas of stiffness accounting for <50 % of the lesion area.

Score 3 – The lesion is mostly stiff, but elastic areas are still present; Stiffness is over >50 % of the lesion area.

Score 4 – Lesion is completely stiff.

After strain elastography, shear wave elastography of the lesion was also performed in the longitudinal plane using Acoustic Radiation Force Impulse (ARFI) technology. Virtual Touch Quantification (VTQ) and Virtual Touch Imaging Quantification (VTIQ) software were used for shear wave elastography assessment. Quantitative analysis was done using the VTQ application. It provides shear wave velocity at the user-defined region of interest (ROI), and two parameters, i.e. Young modulus: in kilopascal (kPa) and Shear wave speed (m/s), were measured. The dynamic range for shear wave velocity measurements was set as 0.5 to 10 m/s. These values were measured three times for each lesion (preferably in the solid parts of the lesion), and the mean value was considered final. VTIQ provides an image-based assessment of shear wave velocity using colour-coded scales (elastogram). It was used to identify stiffness in different areas of the lesions on the basis of their colour coding as follows-Low Stiffness (Blue colour), Intermediate stiffness (Turquoise to yellow) and High stiffness (Red colour). The ultrasound findings were correlated with pathological findings in all the cases.

Statistical Analysis. The acquired data was entered into a Microsoft Excel spreadsheet and subjected to statistical analysis using software SPSS version 20. p-value less than 0.05 was considered significant. Sensitivity, specificity, PPV and NPV were calculated for conventional ultrasound techniques alone & in combination with elastography. The receiver operating characteristic curve, or ROC curve analysis, was done to generate ideal cut-off values for the sonoelastography score, eSie touch, VTQ, and VTIQ to diagnose a lesion as malignant or benign.

3. Results

In the present study, a total of 50 patients were selected as per inclusion and exclusion criteria between the periods of Aug 2021 to Nov 2022. The age of the study population ranged from 16 to 75 years, with a mean age of 38.82 years, where the maximum number of subjects was found in 21 to 30 (38.0 %). 56 % (28 patients) of the patients were female, and the remaining were males (22 patients). According to clinical complaints, the maximum number of patients complained about swelling (76 %), followed by pain (16 %) (Table 1).

Table 1

Distribution of Masses according to the various Demographic Characteristics

Age in Years	No.	%
<20	3	6.0
21-30	19	38.0
31-40	8	16.0
41-50	9	18.0
51-60	4	8.0
>60	7	14.0
Total	50	100.0
Sex	No.	%
Male	22	44.0
Female	28	56.0
Clinical complaints	No.	%
Pain	8	16.0
Pain & swelling	4	8.0
Swelling	38	76.0
Total	50	100.0

Out of the 50 salivary gland lesions included in the study, 44 (88 %) were found to be benign, whereas 6 (12 %) were found to be malignant (Table 2). The two most frequent lesions in the study were Pleomorphic adenoma (60.0 %) and Warthin's Tumor (28 %). (Fig 1, 2).

Table 2

Distribution of cases according to Pathological diagnosis (FNAC)

FNAC Findings	No.	%
Pleomorphic adenoma	30	60.0
Warthin's Tumor	14	28.0
Squamous cell carcinoma	1	2.0
Myoepithelial carcinoma	1	2.0
Metastatic adenocarcinoma	1	2.0
Carcinoma ex-pleomorphic adenoma	1	2.0
Adenoid cystic carcinoma	1	2.0
Acinic cell carcinoma	1	2.0
Total	50	100.0

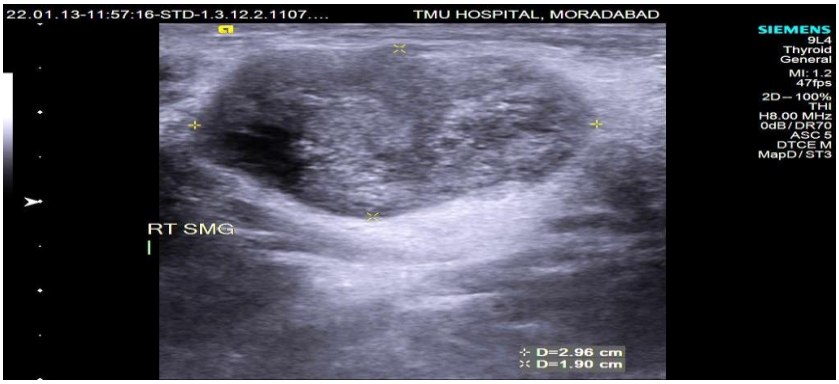

a

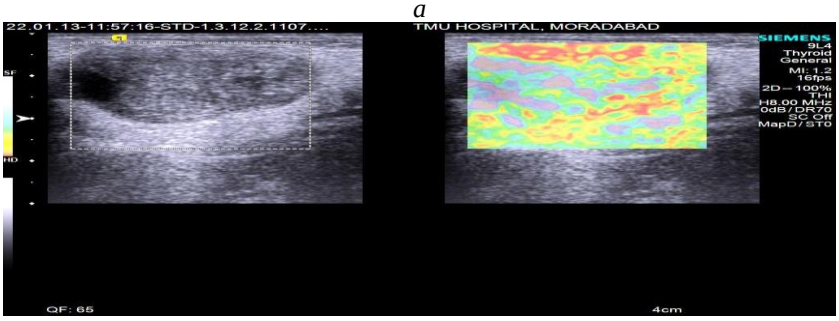

b

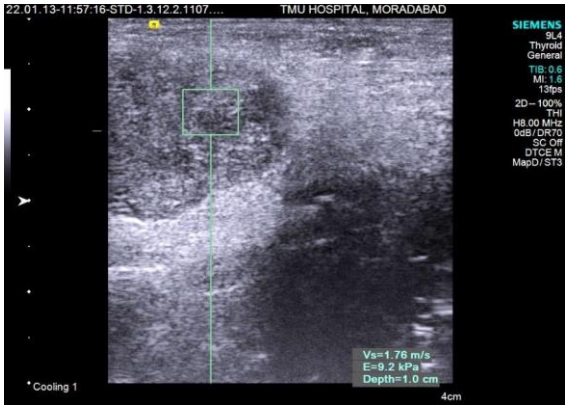

c

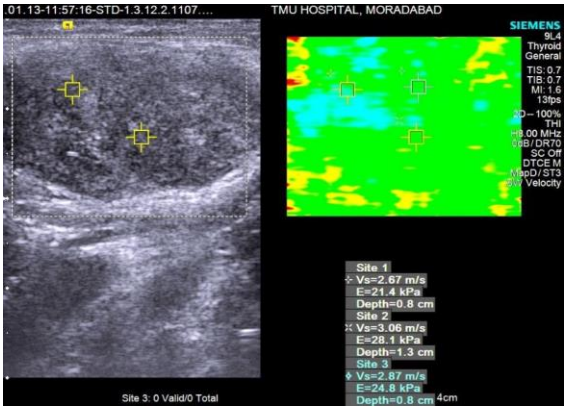

d

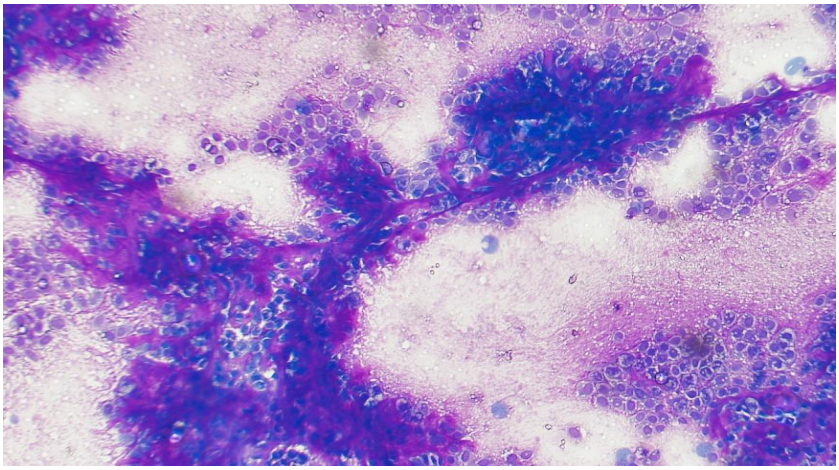

e

Fig. 1. USG and Elastographic findings in a case of Pleomorphic Adenoma: *a* – B mode USG shows a Focal, well-demarcated, oval-shaped, heterogeneously hypoechoic solid lesion in the right submandibular gland; *b* – strain elastography (eSie touch) shows predominantly soft lesion (represented by green & blue colour) with some areas of stiffness (represented by red colour) accounting for <50 % of the lesion area (corresponding to Score 2) indicating low tissue stiffness; *c* – shear wave elastography (VTQ) shows the velocity of 1.76 m/s and stiffness in kPa of 9.2 within the selected ROI; *d* – shear wave elastography (VTIQ) shows variable velocity ranging from 2.67 m/s to 3.06 m/s at multiple ROIs within the lesion; *e* – microphotograph shows poorly cohesive myoepithelial cells with abundant pale cytoplasm and bland nuclei associated with fibrillar fibromyxoid stroma (×200) – Pleomorphic Adenoma

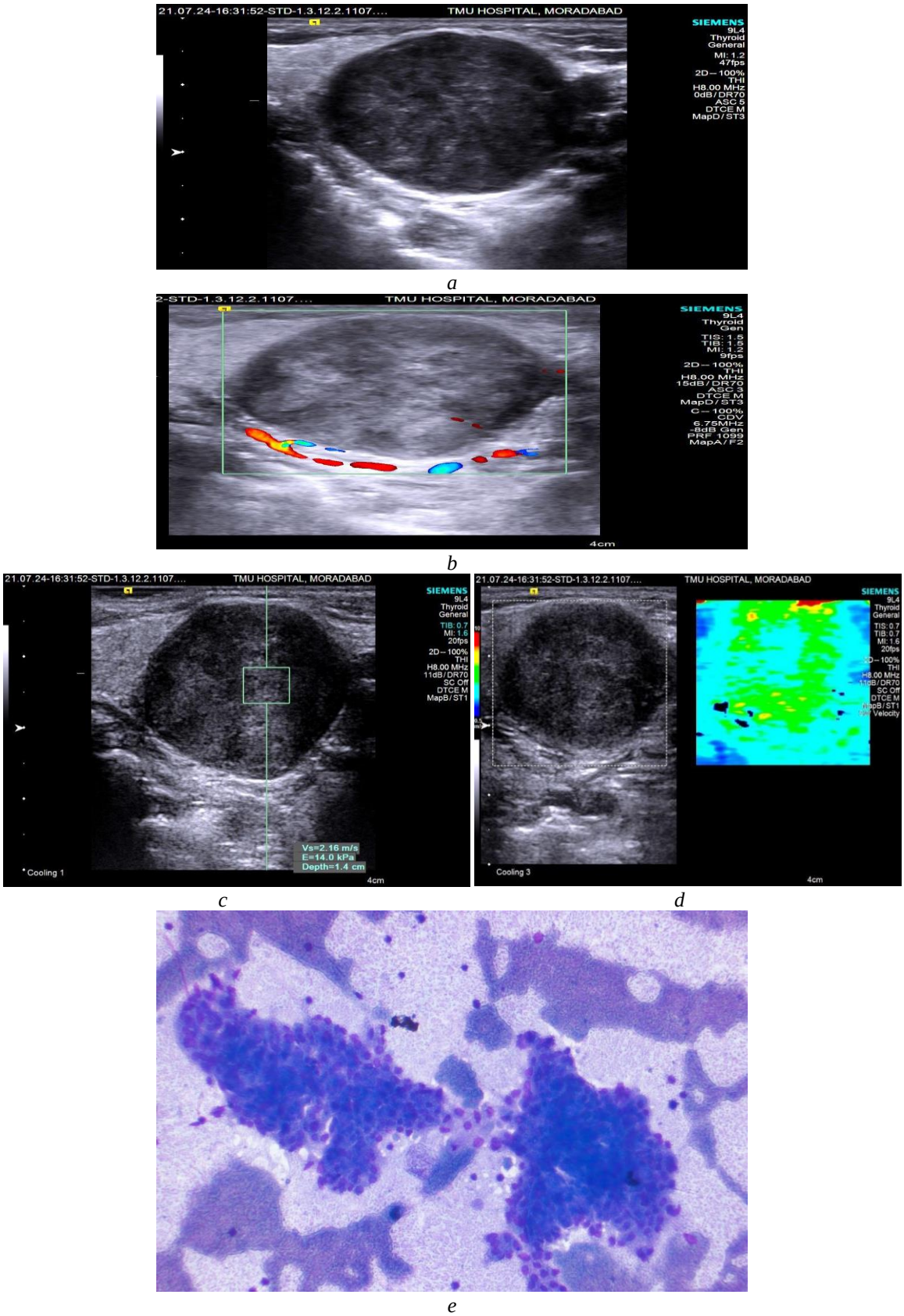

a

b

c *d*

e

Fig. 2. USG and Elastographic findings in a case of Warthin's Tumor: *a* – B mode USG shows a Focal, well-demarcated, round-shaped, heterogeneously hypoechoic solid lesion in the submandibular gland; *b* – colour doppler USG shows a peripheral pattern of vascularity around the lesion; *c* – shear wave elastography (VTQ) shows the velocity of 2.16 m/s & stiffness of 14.0 kPa at the selected ROI; *d* – shear wave elastography (VTIQ) shows colour-coded map representing predominantly low stiffness area (represented by green and blue colour) in the lesion; *e* – microphotograph shows a monolayered sheet of bland oncocytic epithelial cells with scattered lymphocytes on a background of murky fluid (×200) – Warthin's Tumor

The size of the lesion was compared between the Malignant & Benign categories. In Benign and Malignant lesions, the mean size of the long axis was 24.83±9.15 mm and 30.83±9.15 mm, respectively, whereas, for the short axis, these were 18.5±7.14 mm and 23.33 mm, respectively**.** However, the difference in the mean sizes was not statistically significant (Table 3).

Table 4 shows the distribution of various sonomorphological features assessed on the Grayscale and colour doppler amongst the malignant and benign salivary gland lesions.

23 out of 44 purely benign lesions were correctly diagnosed as benign on Conventional USG (Grayscale & Doppler), while the remaining 21 were diagnosed as malignant.

Of the malignant lesions, out of 6 lesions, 4 were correctly diagnosed as malignant, while 2 were falsely labelled as benign (Table 5).

Table 3

The difference in the size of malignant and non-malignant salivary gland lesions

Size of Lesion	FNAC Findings-Benign		FNAC Findings-Malignant		Statistic	
	n	Mean±SD	n	Mean±SD	Difference	P value
Long axis (mm)	44	24.8±9.1	6	30.8±14.3	5.9	0.16*
Short axis (mm)	44	18.5±7.1	6	23.3±12.1	4.8	0.16*

*Note: * – Non-significant*

Table 4

Frequency distribution of cases according to various USG Parameters (Grayscale and Color doppler)

USG Findings		No.	**%**
Type of lesion	Focal	48	96.0
	Diffuse	2	4.0
Shape of lesion	Round	6	12.0
	Oval	20	40.0
	Irregular	12	24.0
	Lobulated	12	24.0
Margin of lesion	Well demarcated	40	80.0
	Poorly demarcated	10	20.0
Consistency of lesion	Solid	26	52.0
	Mixed	24	48.0
Echo pattern of lesion	Hypoechoic	14	28.0
	Mixed	36	72.0
Echotexture of lesion	Homogeneous	13	28.0
	Heterogeneous	37	72.0
Vascularity	Present	42	84.0
	Absent	8	16.0
Vascularity Pattern	Peripheral	16	38.1
	Mixed	11	26.2
	Central	15	35.7

Table 5

Comparison of conventional USG diagnosis with pathological diagnosis in terms of benign and malignant

USG diagnosis	FNAC diagnosis				Total, abs. (%)
	Malignant	%	Benign	%	
Malignant	4	66.7	21	47.7	25 (50.0 %)
Benign	2	33.7	23	52.3	25 (50.0 %)
Total	6	12	44	88	50

When conventional USG was combined with elastography, 35 out of 44 purely benign lesions were correctly diagnosed as benign, while the remaining 9 were diagnosed as malignant. Of the malignant lesions, out of 6 lesions, 5 were correctly diagnosed as malignant, and only 1 was falsely labelled as benign (Table 6).

As can be seen in Table 7, the combination of USG and elastography yielded a higher diagnostic performance as compared to USG alone.

The sonoelastography score (eSie touch) correlation with FNAC showed statistically significant distribution patterns (Table 8).

Similarly, the difference in the mean values for VTQ (kPa), VTQ (m/s), and VTIQ (m/s) in benign and malignant lesions was also found to be statistically significant (Table 9).

The ROC analysis of sonoelastography, VTQ (kPa), VTIQ (m/s) and eSie touch score against FNAC

findings was done to estimate the cut-off value with optimized sensitivity and specificity to diagnose the lesion as malignant or benign. The cut-off value >40.7 was obtained for VTQ (kPa) with 83.33 % sensitivity and 88.64 % specificity. Similarly, for VTIQ (m/s) and eSie touch score, cut-off values were >3.74 and >2, with reasonably good sensitivity and specificity to diagnose the lesion as malignant (Table 10).

Table 6

Comparison of combined USG elastography diagnosis with Pathological diagnosis in terms of benign and malignant

USG & Elasto's diagnosis	FNAC diagnosis				Total, abs. (%)
	Malignant	%	Benign	%	
Malignant	5	83.3	9	20.5	14 (28.0 %)
Benign	1	16.7	35	79.5	36 (72.0 %)
Total	6	12	44	88	50

Table 7

Diagnostic Performance of Conventional USG (USG-CD) and USG-Elastography (USG-CD-Elasto) against FNAC findings to differentiate between malignant & benign

S.No.	Parameters	USG-CD vs FNAC	USG-CD-Elasto vs FNAC
1.	Sensitivity	66.67	83.33
2.	Specificity	52.27	79.55
3.	PPV	16.00	35.71
4.	NPV	92.00	97.22
5.	Accuracy	54.00	80.00

Table 8

Correlation of elastography score (eSie touch) with pathological diagnosis

Elastography score eSie touch	FNAC Findings				Total, abs. (%)
	Malignant	%	Benign	%	
1	1	16.7	5	11.4	6 (12.0 %)
2	0	0.00	30	68.2	30 (60.0 %)
3	2	33.3	9	20.5	11 (22.0 %)
4	3	50	0	0	3 (6.0 %)
5	6	100	44	100	50
χ^2	26.613				
Significance level	$p < 0.0001$				

Table 9

Comparison of VTQ (kPa), VTQ (m/s), and VTIQ (m/s) against FNAC findings to differentiate malignant & benign lesions

Variable	FNAC – Benign		FNAC – Malignant		Statistic	
	n	Mean±SD	n	Mean±SD	Difference	P value
VTQ (kPa)	44	25.4±15.6	6	53.6±25.4	28.1	0.0004*
VTQ (m/s)	44	2.8±0.8	6	4.0±1.1	1.2	0.0011*
VTIQ (m/s)	44	2.9±0.8	6	4.3±1.2	1.3	0.0010*

*Note: * – statistically significant*

Table 10

ROC analysis of criterion values and coordinates of the ROC curve

ROC analysis of Elastographic parameters	VTQ (kPa)	VTIQ	eSie-touch
The area under the ROC curve (AUC)	0.822	0.807	0.809
Significance level P (area=0.5)	0.0191	0.0235	0.0425
Cut-off value	>40.7	>3.74	>2
Sensitivity	83.33	83.33	83.33
Specificity	88.64	88.64	79.55

4. Discussion

Out of the 50 salivary gland lesions included in the study, 44 (88 %) were benign, whereas 6 (12 %) were malignant.

Demographic Profile. Most of the affected patients were between the ages of 21–30 yrs (38 %), and the mean age of the study population was 38.82 yrs. The maximum number of patients in the study by Babu N et al. [25] also belonged to the 21–30 yrs age bracket (39.14 %). The mean age of patients in the study by Dumitru et al. [26] was 44.2 years, which nearly matches our study.

In the present study, the females (56 %) were mostly affected as compared to males (44 %). 63.15 % of females got affected by salivary-gland lesions and out-

numbered males in a study by Dumitriu et al. [26]. Similarly, female predominance (51.9 %) was also observed by Stewart et al. [27] in their study.

Glandular involvement. We found predominant involvement of the parotid gland (PG – 66 %) as compared to the submandibular gland (SMG – 44 %). These findings nearly match the studies of Bocatto et al. [28] (Parotid gland – 87.6 % and submandibular gland – 10.1 %), Rajdeo et al. [29] (PG – 70 % and SMG – 24 %), and Cristallini et al. [30] (PG – 70.8 % and SMG – 21.6 %) in which parotid gland involvement was more frequent than submandibular gland involvement.

The two most prevalent salivary gland lesions, as reported in the literature, are Pleomorphic adenoma and Warthin's tumour [31, 32]. Pleomorphic adenoma was the most frequent tumour comprising 54.2 % of all tumours and 80.3 % of the benign salivary gland tumours in the case series (256 cases) of Kamble RC et al. [32]. In this study, also Pleomorphic adenoma (60 %) was the most frequent lesion, followed by Warthin's tumour (28 %).

Size. We observed no statistically significant difference in gland and lesion size between malignant and benign lesions ($p > 0.05$). These findings are in clear contrast to the findings of Speight P et al. [33] as they stated that the behaviour of salivary tumours was only marginally influenced by histologic type while greatly influenced by lesion size. This possible reason for this discrepancy may be attributed to the low number of malignant cases in the present study.

Sonographic features. Malignant and benign cases were identified according to the elastography score (eSie touch). We were not able to differentiate between benign and malignant lesions based on the scores alone. Dumitriu et al. [26] evaluated salivary-gland tumours using elastography. They got higher scores for malignant tumours than benign tumours. In 2011, Dumitriu et al. [5] used the same scoring pattern to distinguish between the malignant and benign nature of lesions, but the findings were not statistically significant. Although most malignant masses in their study either scored 3 or 4, few either scored 1 or 2. Also, among tumours with a score of 4, more than half were pleomorphic adenomas [5].

The conventional sonographic features (USG-CD) of malignant salivary-gland lesions consist of irregular form, poorly demarcated outline, heterogeneous echotexture, mixed consistency of lesion and echo pattern, and mixed/central vascularity pattern [34–37]. Whereas not a single parameter is sufficient for adequate diagnostic assessment, so we prepared overall findings for USG-CD while in the case of USG-Color Doppler-Elastography (USG-CD-Elasto), scores of eSie touch, VTQ (kPa), and VTIQ (m/s) were used to prepare overall findings. Further, we validated the overall findings of USG-CD and USG-CD-Elasto for the confirmation of benign and malignant salivary-gland lesions against FNAC findings.

In comparison, the USG-CD diagnosis with FNAC shows that 23 out of

44 purely benign lesions were also diagnosed as benign in the USG-CD findings, while the remaining 21 were misdiagnosed as malignant. In the case of malignant lesions, the USG-CD incorrectly diagnosed four of six lesions as malignant and two as benign. USG-CD-Elasto diagnosis with FNAC shows that 35 out of 44 purely benign lesions were diagnosed as benign in the USG-CD-Elasto finding, while the remaining nine were misdiagnosed as malignant. In the case of malignant lesions, out of 6 lesions, 5 were diagnosed as malignant, and only 1 was falsely diagnosed as benign in USG-CD-Elasto. These findings were utilized to compare the diagnostic performances of USG-CD and USG-CD-Elasto, and their sensitivity, specificity, PPV, NPV, and accuracy were determined. The USG-CD-Elasto showed higher diagnostic performance with 83.33 % sensitivity, 79.55 % specificity, 35.71 % PPV, 97.22 % NPV, and 80.00 % accuracy as compared to conventional ultrasound techniques.

Cheng et al. [38] also reported similar enhanced diagnostic performance after the addition of sonoelastography to conventional USG, with 89 % specificity and 85 % accuracy. A German-based meta-analysis reported 92 % sensitivity and 90 % specificity in distinguishing benign lesions from malignant ones [39]. Several other studies [40, 41] also suggested that sonoelastography is an independent method capable of assessing malignancy with comparable accuracy to USG. In the study of Cantisani et al. [40], forty of the lesions analyzed harboured a malignant lesion, and US elastography demonstrated that malignant lesions had significantly higher stiffness with respect to benign one**s.** We also observed that sonoelastography provides an add-on capability to USG-Color Doppler to differentiate benign from malignant tumours.

To confirm whether sonoelastography can be used independently to distinguish benign from malignant tissue, we performed ROC analysis, determining criterion values and different ROC curve coordinates. Shear wave velocity (SWV), which is mostly determined by the target tissue's stiffness, is given an objective numerical value by VTQ, while VTIQ, an upgraded technology of VTQ, gives a more inside picture with increased reliability and reproducibility and a smaller ROI with a wide spectrum range. eSie Touch is a relatively new technology for elasticity imaging [42–44].

We compared sonoelastography scores, VTQ (kPa), VTQ (m/s), and VTIQ (m/s), against FNAC-confirmed cases to differentiate between malignant and benign lesions. The difference in VTQ (kPa), VTQ (m/s), and VTIQ (m/s) were statistically significant in all cases because the observed p-values were 0.05. Our findings concord with previous reports [38, 45–47] that stated that the mean value for elasticity (as a measure of stiffness) proved higher in malignant lesions with respect to benign tissue. Cheng et al. [38] found a significant difference in the standard deviation of elasticity between benign and malignant tumours (median±IQR, 25.9±25 vs 34.8± ±20.4 kPa). The standard deviation of elasticity among malignant tumours, pleomorphic adenoma and other benign tumours also showed a significant difference under the Kruskal-Wallis test (median±IQR, 34.8±20.4, 28±22.4, 27.7±20.5, and 13.7±26.4 kPa).

The mean elasticity score was 4.1±0.9 for malignant lesions and 2.1±1.0 for benign lesions in the study by Schaefer et al. [45]. Similarly, Yi et al. [46] also found a higher mean elasticity score for malignant lesions as compared to benign lesions (2.94±1.10 vs 1.78±0.81). Chen et al. [47] reported that for all sizes, Shear wave velocity VTQ and shear wave velocity VTIQ were higher for malignant versus benign tumours ($P<0.05$).

Further, we analyzed the diagnostic performance of sonoelastography scores. The ideal cut-off value generated a ROC curve based on maximum sensitivity and specificity. The specific cut-off scores for the sonoelastography score, eSie touch, VTQ, and VTIQ were determined for FNAC findings to diagnose a lesion as malignant or benign. The cut-off value of >40.7 kPa was obtained for VTQ (kPa) with 83.33 % sensitivity, 88.64 % specificity, and a good AUC value (0.822). Similarly, for VTIQ (m/s) and eSie touch score, cut-off values were >3.74 m/s and >2 scores, with 83.33 % and 83.33 % sensitivity and 88.64 % and 79.55 % specificity with good AUC values (0.807 and 0.809).

Interestingly, Cheng et al. and Chen et al. have also observed similar findings [38, 47]. Chen et al. [38] discovered that the respective cut-off values for VTQ and VTIQ ranged from 2.94 m/s to 4.59 m/s, with sensitivities and specificities ranging from 75 % to 92.59 % and 75 % to 91.84 %, respectively, for different tumour sizes (10, 10-20, and >20 mm).

Similarly, Cheng et al. [47] also observed an optimal cut-off value of 31.5 kPa, and the sensitivity, specificity, and accuracy were 74 %, 62 %, and 64 %, respectively, to differentiate a lesion as malignant or benign. Farasat et al. [3] also observed similar findings (sensitivity 71 % and specificity 50 %) to our study.

Study limitations. Most of the study period coincided with the Covid Pandemic, and as the number of patients presenting to Covid Hospital for salivary abnormalities was limited, the assessment was constrained, which resulted in a smaller sample size than expected.

Prospects for further research. Thus, further research with a larger sample size is warranted to reaffirm the findings of this study.

5. Conclusions

We investigated the role of sonoelastography in the diagnosis of salivary gland tumours, and the following conclusions can be drawn from the study:

1. The elastographic score VTQ (kPa), VTQ (m/s), and VTIQ (m/s) of malignant salivary gland tumours (53.63±25.49, 4.09±1.15, and 4.34±1.26) were greater than those of benign tumours (25.46±0.81, 2.80±0.81 and 2.96±0.84) and the accuracy for identifying malignancy was reasonably good.

2. The ROC curve analysis of VTQ (kPa), VTIQ (m/s) and eSie touch score for differentiating benign from malignant salivary gland lesions demonstrated cut-off values of >40.7, >3.74 and >2, respectively, with fairly good sensitivity and specificity.

3. The combination of USG elastography showed higher diagnostic performance (83.33 % sensitivity, 79.55 % specificity and 80 % accuracy) as compared to conventional USG alone (66.67 % sensitivity, 52.27 % specificity and 54 % accuracy).

4. We propose that the elastographic scores and cut-off values for elasticity obtained might be utilized to aid in the better characterization of salivary gland lesions as benign or malignant. However, elastographic results in malignant & benign tumours may overlap, and thus, sonoelastography alone cannot be relied upon solely. Thus, conventional ultrasound should be combined with sonoelastography in a diagnostic system to achieve better differentiation of benign and malignant salivary gland lesions.

Conflict of interest

The authors declare that they have no conflict of interest in relation to this research, whether financial, personal, authorship or otherwise, that could affect the research and its results presented in this article.

Funding

The study was performed without financial support.

Data availability

Available on reasonable request.

References

1. Agrawal, R. V., Solanki, B. R., Junnarkar, R. V. (1967). Salivary gland tumours. Indian Journal of Cancer, 4 (2), 209–213.

2. Elbeblawy, Y. M., Eshaq Amer Mohamed, M. (2020). Strain and shear wave ultrasound elastography in evaluation of chronic inflammatory disorders of major salivary glands. Dentomaxillofacial Radiology, 49 (3). doi: https://doi.org/10.1259/dmfr.20190225

3. Farasat, M., Yilmaz Ovali, G., Duzgun, F., Eskiizmir, G., Tarhan, S., Tan, A. (2017). Sonoelastographic Features of Major Salivary Gland Tumors and Pathology Correlation. Iranian Journal of Radiology, 15 (1). doi: https://doi.org/10.5812/iranjradiol.64039

4. Mantsopoulos, K., Klintworth, N., Iro, H., Bozzato, A. (2015). Applicability of Shear Wave Elastography of the Major Salivary Glands: Values in Healthy Patients and Effects of Gender, Smoking and Pre-Compression. Ultrasound in Medicine & Biology, 41 (9), 2310–2318. doi: https://doi.org/10.1016/j.ultrasmedbio.2015.04.015

5. Dumitriu, D., Dudea, S., Botar-Jid, C., Băciuţ, M., Băciuţ, G. (2011). Real-Time Sonoelastography of Major Salivary Gland Tumors. American Journal of Roentgenology, 197 (5), W924–W930. doi: https://doi.org/10.2214/ajr.11.6529

6. Zhang, Y.-F., Li, H., Wang, X.-M., Cai, Y.-F. (2018). Sonoelastography for differential diagnosis between malignant and benign parotid lesions: a meta-analysis. European Radiology, 29 (2), 725–735. doi: https://doi.org/10.1007/s00330-018-5609-6

7. Celebi, I., Mahmutoglu, A. S. (2013). Early results of real-time qualitative sonoelastography in the evaluation of parotid gland masses: A study with histopathological correlation. Acta Radiologica, 54 (1), 35–41. doi: https://doi.org/10.1258/ar.2012.120405

8. Altinbas, N. K., Gundogdu Anamurluoglu, E., Oz, I. I., Yuce, C., Yagci, C., Ustuner, E., Akyar, S. (2016). Real-Time Sonoelastography of Parotid Gland Tumors. Journal of Ultrasound in Medicine, 36 (1), 77–87. doi: https://doi.org/10.7863/ultra.16.02038

9. Bagri, N., Misra, R. N., Bajaj, S. K., Chandra, R., Malik, A., Bharadwaj, N., Gaikwad, V. (2020). Evaluation of Salivary Gland Lesions by Real Time Sonoelastography: Diagnostic Efficacy and Comparative Analysis with Conventional Sonography. Journal of Clinical and Diagnostic Research, 14 (6), TC05–TC09. doi: https://doi.org/10.7860/jcdr/2020/43476.13796

10. Cortcu, S., Elmali, M., Tanrivermis Sayit, A., Terzi, Y. (2018). The Role of Real-Time Sonoelastography in the Differentiation of Benign From Malignant Parotid Gland Tumors. Ultrasound Quarterly, 34 (2), 52–57. doi: https://doi.org/10.1097/ruq.0000000000000323

11. Bozzato, A., Zenk, J., Greess, H., Hornung, J., Gottwald, F., Rabe, C., Iro, H. (2007). Potential of ultrasound diagnosis for parotid tumors: Analysis of qualitative and quantitative parameters. Otolaryngology–Head and Neck Surgery, 137 (4), 642–646. doi: https://doi.org/10.1016/j.otohns.2007.05.062

12. Sarvazyan, A. P., Rudenko, O. V., Swanson, S. D., Fowlkes, J. B., Emelianov, S. Y. (1998). Shear wave elasticity imaging: a new ultrasonic technology of medical diagnostics. Ultrasound in Medicine & Biology, 24 (9), 1419–1435. https://doi.org/10.1016/s0301-5629(98)00110-0

13. Nightingale, K., McAleavey, S., Trahey, G. (2003). Shear-wave generation using acoustic radiation force: in vivo and ex vivo results. Ultrasound in Medicine & Biology, 29 (12), 1715–1723. doi: https://doi.org/10.1016/j.ultrasmedbio.2003.08.008

14. Sarvazyan, A., J. Hall, T., W. Urban, M., Fatemi, M., R. Aglyamov, S., S. Garra, B. (2011). An Overview of Elastography-An Emerging Branch of Medical Imaging. Current Medical Imaging Reviews, 7 (4), 255–282. doi: https://doi.org/10.2174/157340511798038684

15. Lerner, R. M., Parker, K. J., Holen, J., Gramiak, R., Waag, R. C. (1988). Sono-Elasticity: Medical Elasticity Images Derived from Ultrasound Signals in Mechanically Vibrated Targets. Acoustical Imaging, 317–327. doi: https://doi.org/10.1007/978-1-4613-0725-9_31

16. Zaleska-Dorobisz, U., Kaczorowski, K., Pawluś, A., Puchalska, A., Inglot, M. (2014). Ultrasound Elastography – Review of Techniques and its Clinical Applications. Advances in Clinical and Experimental Medicine, 23, 645–655. doi: https://doi.org/10.17219/acem/26301

17. Itoh, A., Ueno, E., Tohno, E., Kamma, H., Takahashi, H., Shiina, T. et al. (2006). Breast Disease: Clinical Application of US Elastography for Diagnosis. Radiology, 239 (2), 341–350. doi: https://doi.org/10.1148/radiol.2391041676

18. Karaman, C. Z., Başak, S., Polat, Y. D., Ünsal, A., Taşkın, F., Kaya, E., Günel, C. (2018). The Role of Real-Time Elastography in the Differential Diagnosis of Salivary Gland Tumors. Journal of Ultrasound in Medicine, 38 (7), 1677–1683. doi: https://doi.org/10.1002/jum.14851

19. Yerli, H., Yilmaz, T., Kaskati, T., Gulay, H. (2011). Qualitative and Semiquantitative Evaluations of Solid Breast Lesions by Sonoelastography. Journal of Ultrasound in Medicine, 30 (2), 179–186. doi: https://doi.org/10.7863/jum.2011.30.2.179

20. Dejaco, C., De Zordo, T., Heber, D., Hartung, W., Lipp, R., Lutfi, A. et al. (2014). Real-Time Sonoelastography of Salivary Glands for Diagnosis and Functional Assessment of Primary Sjögren's Syndrome. Ultrasound in Medicine & Biology, 40 (12), 2759–2767. doi: https://doi.org/10.1016/j.ultrasmedbio.2014.06.023

21. Khalife, A., Bakhshaee, M., Davachi, B., Mashhadi, L., Khazaeni, K. (2016). The diagnostic value of B-mode sonography in differentiation of malignant and benign tumors of the parotid gland. Iranian Journal of Otorhinolaryngology, 28 (5), 305–312.

22. Bialek, E. J., Jakubowski, W., Szczepanik, A. B., Maryniak, R. K., Prochorec-Sobieszek, M., Bilski, R., Szopinski, K. T. (2007). Vascular patterns in superficial lymphomatous lymph nodes: A detailed sonographic analysis. Journal of Ultrasound, 10 (3), 128–134. doi: https://doi.org/10.1016/j.jus.2007.06.003

23. Na, D. G., Lim, H. K., Byun, H. S., Kim, H. D., Ko, Y. H., Baek, J. H. (1997). Differential diagnosis of cervical lymphadenopathy: usefulness of color Doppler sonography. American Journal of Roentgenology, 168 (5), 1311–1316. doi: https://doi.org/10.2214/ajr.168.5.9129432

24. Zengel, P., Notter, F., Clevert, D. A. (2019). VTIQ and VTQ in combination with B-mode and color Doppler ultrasound improve classification of salivary gland tumors, especially for inexperienced physicians. Clinical Hemorheology and Microcirculation, 70 (4), 457–466. doi: https://doi.org/10.3233/ch-189312

25. Babu N., S., Mahadev, N. H., V., K. G. (2019). A clinical study of the incidence of salivary gland tumors in a tertiary care teaching hospital. International Surgery Journal, 6 (6), 2110. doi: https://doi.org/10.18203/2349-2902.isj20192376

26. Dumitriu, D., Dudea, S., Badea, R., Baciut, G., Baciut, M. (2008). B-mode and Doppler ultrasound appearance of salivary gland tumors. Ultraschall in Der Medizin - European Journal of Ultrasound, 29 (S1), 31–37. doi: https://doi.org/10.1055/s-2008-1079890

27. Stewart, C. J. R., MacKenzie, K., McGarry, G. W., Mowat, A. (2000). Fine-needle aspiration cytology of salivary gland: A review of 341 cases. Diagnostic Cytopathology, 22 (3), 139–146. doi: https://doi.org/10.1002/(sici)1097-0339(20000301)22:3<139::aid-dc2>3.0.co;2-a

28. Boccato, P., Altavilla, G., Blandamura, S. (1998). Fine Needle Aspiration Biopsy of Salivary Gland Lesions. Acta Cytologica, 42 (4), 888–898. doi: https://doi.org/10.1159/000331964

29. Rajdeo, R., Shrivastava, A., Bajaj, J., Shrikhande, A., Rajdeo, R. (2015). Clinicopathological study of salivary gland tumors: An observation in tertiary hospital of central India. International Journal of Research in Medical Sciences, 1691–1696. doi: https://doi.org/10.18203/2320-6012.ijrms20150253

30. Cristallini, E. G., Ascani, S., Farabi, R., Liberati, F., Macciò, T., Peciarolo, A., Bolis, G. B. (1997). Fine Needle Aspiration Biopsy of Salivary Gland, 1985–1995. Acta Cytologica, 41 (5), 1421–1425. doi: https://doi.org/10.1159/000332853

31. Ito, F. A., Ito, K., Vargas, P. A., de Almeida, O. P., Lopes, M. A. (2005). Salivary gland tumors in a Brazilian population: a retrospective study of 496 cases. International Journal of Oral and Maxillofacial Surgery, 34 (5), 533–536. doi: https://doi.org/10.1016/j.ijom.2005.02.005

32. Joshi, A. N., Kamble, R. C., Mestry, P. J. (2013). Ultrasound Characterization of Salivary Lesions. An International Journal of Otorhinolaryngology Clinics, 5 (4), 16–29. doi: https://doi.org/10.5005/aijoc-5-4-16

33. Speight, P., Barrett, A. (2002). Salivary gland tumours. Oral Diseases, 8 (5), 229–240. doi: https://doi.org/10.1034/j.1601-0825.2002.02870.x

34. Wu, S., Liu, G., Chen, R., Guan, Y. (2012). Role of ultrasound in the assessment of benignity and malignancy of parotid masses. Dentomaxillofacial Radiology, 41 (2), 131–135. doi: https://doi.org/10.1259/dmfr/60907848

35. Singh, S., Nagar, A., Sakhi, P., Kataria, S., Julka, K., Gupta, A. (2015). Role of high resolution sonography in characterization of solid salivary gland tumors. Journal of Evolution of Medical and Dental Sciences, 4 (39), 6787–6792. doi: https://doi.org/10.14260/jemds/2015/984

36. Lo, W., Chang, C., Wang, C., Cheng, P., Liao, L. (2020). A Novel Sonographic Scoring Model in the Prediction of Major Salivary Gland Tumors. The Laryngoscope, 131 (1), E157–E162. doi: https://doi.org/10.1002/lary.28591

37. Bialek, E. J., Jakubowski, W., Zajkowski, P., Szopinski, K. T., Osmolski, A. (2006). US of the Major Salivary Glands: Anatomy and Spatial Relationships, Pathologic Conditions, and Pitfalls. RadioGraphics, 26 (3), 745–763. doi: https://doi.org/10.1148/rg.263055024

38. Cheng, P.-C., Lo, W.-C., Chang, C.-M., Wen, M.-H., Cheng, P.-W., Liao, L.-J. (2022). Comparisons among the Ultrasonography Prediction Model, Real-Time and Shear Wave Elastography in the Evaluation of Major Salivary Gland Tumors. Diagnostics, 12 (10), 2488. doi: https://doi.org/10.3390/diagnostics12102488

39. Bojunga, J., Herrmann, E., Meyer, G., Weber, S., Zeuzem, S., Friedrich-Rust, M. (2010). Real-Time Elastography for the Differentiation of Benign and Malignant Thyroid Nodules: A Meta-Analysis. Thyroid, 20 (10), 1145–1150. doi: https://doi.org/10.1089/thy.2010.0079

40. Cantisani, V., Ulisse, S., Guaitoli, E., De Vito, C., Caruso, R., Mocini, R. et al. (2012). Q-Elastography in the Presurgical Diagnosis of Thyroid Nodules with Indeterminate Cytology. PLoS ONE, 7 (11), e50725. doi: https://doi.org/10.1371/journal.pone.0050725

41. Zhang, Y.-F., Xu, H.-X., He, Y., Liu, C., Guo, L.-H., Liu, L.-N., Xu, J.-M. (2012). Virtual Touch Tissue Quantification of Acoustic Radiation Force Impulse: A New Ultrasound Elastic Imaging in the Diagnosis of Thyroid Nodules. PLoS ONE, 7 (11), e49094. doi: https://doi.org/10.1371/journal.pone.0049094

42. Cho, S. H., Lee, J. Y., Han, J. K., Choi, B. I. (2010). Acoustic Radiation Force Impulse Elastography for the Evaluation of Focal Solid Hepatic Lesions: Preliminary Findings. Ultrasound in Medicine & Biology, 36 (2), 202–208. doi: https://doi.org/10.1016/j.ultrasmedbio.2009.10.009

43. Golatta, M., Schweitzer-Martin, M., Harcos, A., Schott, S., Gomez, C., Stieber, A. et al. (2014). Evaluation of Virtual Touch Tissue Imaging Quantification, a New Shear Wave Velocity Imaging Method, for Breast Lesion Assessment by Ultrasound. BioMed Research International, 2014, 1–7. doi: https://doi.org/10.1155/2014/960262

44. Fahey, B. J., Nelson, R. C., Bradway, D. P., Hsu, S. J., Dumont, D. M., Trahey, G. E. (2007). In vivo visualization of abdominal malignancies with acoustic radiation force elastography. Physics in Medicine & Biology, 53 (1), 279–293. doi: https://doi.org/10.1088/0031-9155/53/1/020

45. Schaefer, F. K. W., Heer, I., Schaefer, P. J., Mundhenke, C., Osterholz, S., Order, B. M. et al. (2011). Breast ultrasound elastography—Results of 193 breast lesions in a prospective study with histopathologic correlation. European Journal of Radiology, 77 (3), 450–456. doi: https://doi.org/10.1016/j.ejrad.2009.08.026

46. Yi, A., Cho, N., Chang, J. M., Koo, H. R., La Yun, B., Moon, W. K. (2011). Sonoelastography for 1786 non-palpable breast masses: diagnostic value in the decision to biopsy. European Radiology, 22 (5), 1033–1040. doi: https://doi.org/10.1007/s00330-011-2341-x

47. Chen, Y., Han, T., Wu, R., Yao, M., Xu, G., Zhao, L. et al. (2016). Comparison of Virtual Touch Tissue Quantification and Virtual Touch Tissue Imaging Quantification for diagnosis of solid breast tumors of different sizes. Clinical Hemorheology and Microcirculation, 64 (2), 235–244. doi: https://doi.org/10.3233/ch-16192

Received date 13.12.2022
Accepted date 26.01.2023
Published date 31.01.2023

Arpit Deriya, Resident, Department of Radiodiagnosis, Teerthanker Mahaveer Medical College & Research Centre, Moradabad, Uttar Pradesh, India, 244001

Deepti Arora*, Associate Professor, Department of Pathology, Teerthanker Mahaveer Medical College & Research Centre, Moradabad, Uttar Pradesh, India, 244001

Ankur Malhotra, Professor, Department of Radiodiagnosis, Teerthanker Mahaveer Medical College & Research Centre, Moradabad, Uttar Pradesh, India, 244001

Shruti Chandak, Professor, Department of Radiodiagnosis, Teerthanker Mahaveer Medical College & Research Centre, Moradabad, Uttar Pradesh, India, 244001

Vaibhav Goyal, Resident, Department of Radio-diagnosis, Teerthanker Mahaveer Medical College & Research Centre, Moradabad, Uttar Pradesh, India, 244001

Paurush Jain, Resident, Department of Radiodiagnosis, Teerthanker Mahaveer Medical College & Research Centre, Moradabad, Uttar Pradesh, India, 244001

***Corresponding author:** *Deepti Arora, e-mail: deepti.a15@gmail.com*